Kinetics and Thermodynamics of the Assembly of the Parallel- and Antiparallel-Packed Sections of Synthetic Thick Filaments of Skeletal Myosin: A Pressure-Jump Study†

Julien S. Davis*

Department of Biochemistry, University of the Witwatersrand, Johannesburg 2001, South Africa

Received January 29, 1985

ABSTRACT: Earlier work on the length regulation mechanism of synthetic myosin filaments generated at pH 8.2 showed the process to be mediated through the dissociation rate constant which had an increasing and apparently monophasic exponential dependence on filament length and an association rate constant that was length independent, filament growth ceasing at the point of equilibrium [Davis, J. S. (1981) *Biochem. J. 197*, 309–314]. In this work, the exponential dependence of the dissociation rate constant on thick filament length was shown to be more complex than originally thought. Two phases were resolved, one of which correlated with the dissociation of parallel-packed myosin and the other with that of antiparallel-packed material. The pressure dependence of the dissociation reaction for the parallel-packed material showed that the activation volume decreased linearly with length while the Gibbs energy increased. This was interpreted as indicating that the weakening of the interaction between dimer and filament with length was accompanied by a decrease in the extent of ionic bonding. The case in the antiparallel-packed region was quite different, with the activation volume and the Gibbs energy both increasing linearly. The contribution from ionic bonding thus rises counter to the change in Gibbs energy, presumably at the expense of other noncovalent interactions. The relationship between the synthetic thick filaments and their in vivo counterparts is also considered in some detail.

The assembly of purified myosin into synthetic thick filaments provides an excellent system in which to study the way in which a protein polymer of complex structure and controlled size is derived wholly from the polymerization of a single type of subunit. Studies on the mechanism have proved it to belong to a class separate from other polymerizing systems that are regulated either by externally introduced information (copolymerizing proteins etc.) or by simple geometrically imposed constraints on polymer size (icosahedral viral coats and subunit enzymes) (Davis, 1981c, 1983). Myosin thick filament assembly relies solely on *emergent properties* for size regulation and for the sequential generation of its complex bipolar structure. Mechanisms of this type have been proposed in the past (Kellenberger, 1969), but the myosin system has been the first to yield to a detailed mechanistic study.

Pressure-jump kinetic studies by Davis and co-workers (Davis, 1981a,b; Davis et al., 1982) have shown that the growth of the thick filament from either side of the bare zone (the propagation reaction) occurs through the strictly sequential addition to the two growing ends of the bipolar thick filament of a head to tail myosin dimer with a subunit axial stagger of 44 nm. The assembly rate constant for the addition of dimer was found to be independent of filament length. The dissociation rate constant, by way of contrast, increases exponentially by a factor of ±500 as the filament grows bidirectionally from the central bare zone (the antiparallel-packed zone to either side of the 2-fold rotational axis of symmetry) out to its full length. Filament growth ceases at the point of equilibrium between the "on" and "off" rates, thus generating the characteristic narrow length distribution seen in electron micrographs.

For this work to be relevant to native thick-filament assembly, the particular class of synthetic filaments used for these experiments should have the same underlying structure and molecular interactions (excluding the contribution from the copolymerizing proteins) as their in vivo counterparts. A number of morphologically distinct classes of thick filament can be generated from purified myosin by changing the pH of the solvent (Josephs & Harrington, 1966). The particular class of filament used in these experiments is generated between pH 8.0 and 8.5 at 5 °C and characteristically has the appearance of a homogeneous population of polymers shorter in length but otherwise structurally similar to their native counterparts (Josephs & Harrington, 1968). However, a considerable amount of experimental work has been done on a different class of filaments generated at pH 7.0 and 5 °C, conditions which generally result in the formation of a heterogeneous population of polymers of length similar to that of native thick filaments but otherwise dissimilar in that they are thicker than native filaments and in a number of instances lack a discernible central bare zone (Josephs & Harrington, 1966). Evidence is presented under Discussion to further support the contention that filaments generated at pH 8.2 at 5 °C are closer in terms of their molecular interactions to the physiological state (pH 7.2 at 40 °C) than the class of filaments generated at pH 7.0 and 5 °C.

The work presented in this paper was prompted by the observation that the exponential dependence of the dissociation rate constant on filament length was in fact more complex than the original monophasic dependency indicated; one phase appears to be correlated with parallel-packed myosin and the other with antiparallel-packed material. The dependence of the Gibbs energy (ΔG°) and activation volume (ΔV^*) on

† This work was supported by the Vice Chancellor's Research Award of the University and by the Council for Scientific and Industrial Research.

* Address correspondence to this author at the Department of Biology, The Johns Hopkins University, Baltimore, MD 21218.

0006-2960/85/0424-5263$01.50/0

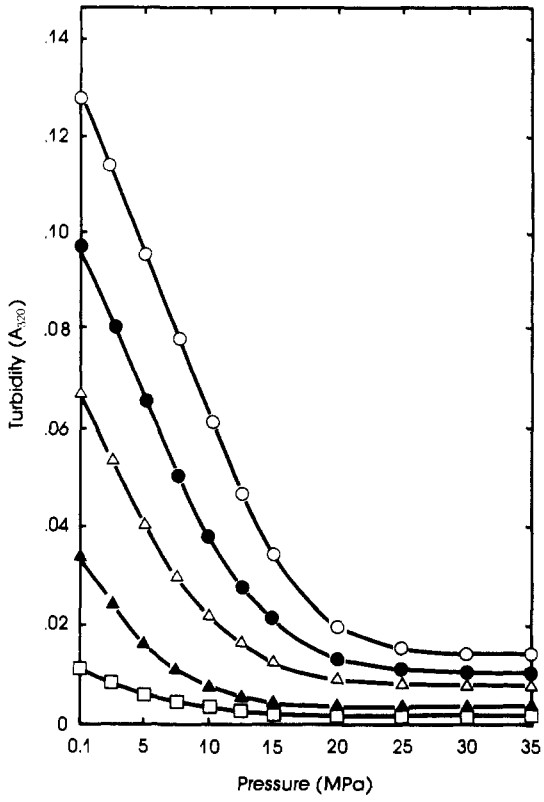

FIGURE 1: Effect of hydrostatic pressure on the thick filament self-assembly equilibrium at different protein concentrations. Total myosin concentrations were (○) 1, (●) 0.8, (△) 0.6, (▲) 0.4, and (□) 0.2 mg/mL.

filament length is investigated in order to give an insight into the way in which the intersubunit bonding domains change in the length-dependent manner. To obtain the $\Delta G°$ and $\Delta V°$ values associated with parallel- and antiparallel-packed myosin, the pressure dependencies of the strength of the cooperativity of assembly and the overall rate of dissociation are analyzed, and the implications of the results for filament length control are discussed.

Experimental Procedures

Preparation of Myosin. Myosin was obtained from the back and hind leg muscles of a rabbit. The purification procedure included ammonium sulfate fractionation and finally chromatography on Sephadex A-50 (Starr & Offer, 1971). A specific fraction of the column eluate was used for the experiments (Davis, 1981a).

Preparation of Filaments. Filaments were generated by two 16-h dialyses against 0.15 M KCl–0.01 M Bicine [*N*,*N*-bis-(2-hydroxyethyl)glycine] buffer, pH 8.2, at 5 °C (Davis, 1981a).

Electron Microscopy. The filaments were cross-linked with glutaraldehyde, stained on a carbon film with 2% uranyl acetate solution, washed once, and viewed in a JEM 100S electron microscope (Davis, 1981a).

Pressure-Jump Apparatus. The instruments used are described elsewhere as follows: the downward pressure jump (Davis & Gutfreund, 1976); the upward pressure-jump (Davis, 1982); the instrument electronics and optics (Davis, 1981a); and the data collection and computing facility (Davis, 1981b).

Results

Pressure Dependence of the Thick Filament Equilibrium. The equilibrium experiments are primarily used to establish the pressures and myosin concentrations at which one can

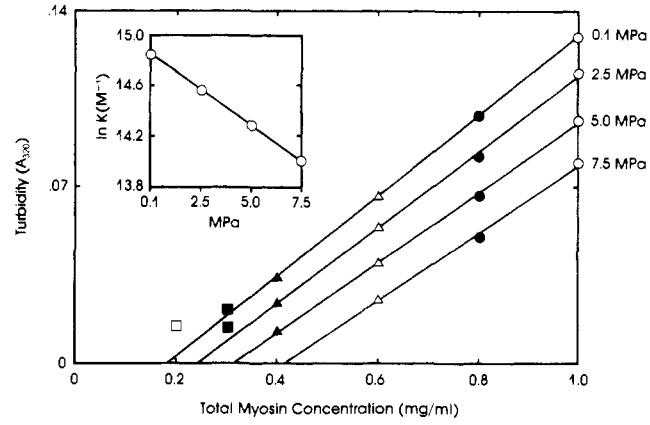

FIGURE 2: Effect of total myosin concentration on filament turbidity at various pressures. The graph is essentially a replot of the first linear phase of Figure 1 and uses a similar set of symbols except for the additional 0.3 mg/mL. The inset graph shows the plot used to obtained the ΔV of −276 cm^3 mol^{-1} for the dissociation of filament into nonfilamentous myosin.

expect the filaments to be fully dissociated and to provide an overall reaction volume (ΔV) for the process from the pressure dependence of the critical concentration. The specific turbidity for the incorporation of myosin into the parallel-packed part of the thick filament was also determined (Davis, 1981a). The characterization of the system in this way is necessary as minor changes in solvent conditions can have a significant effect on these parameters.

It can be seen from Figure 1 that the filaments are fully dissociated at pressures in excess of 27.5 MPa (275 atm) for all the myosin concentrations used. The slope of the plot of the turbidity (A_{320}) vs. concentration data at atmospheric pressure yielded a specific turbidity ($A^{1\%}_{320}$) of 1.59 for the reaction. The linearity of the plot obviates the need to correct for filament nonideality over the concentration range used. A molecular weight of 513 000 [M. Elzinga quoted by Cooper & Trinick (1984)] rather than the 465 000 used in our earlier papers results in a molar turbidity value of 8.16×10^4 mol^{-1} cm^{-1}. In kinetic experiments, a correction has to be made on a stoichiometric basis for the turbidity signal from the product (Davis, 1981b). Using an $A^{1\%}_{320}$ of 0.9 for nonfilamentous myosin, the corrected specific turbidity is then $8.16 \times 10^4 - 4.62 \times 10^3 = 7.79 \times 10^4$ mol^{-1} cm^{-1}.

The critical concentrations at various pressures are obtained from the intercepts of the various isobaric plots and the concentration axis of Figure 2. These values are raised by 6% to correct for the turbidity contribution from nonfilamentous myosin (Davis, 1981b). The ΔV of −264 cm^3 mol^{-1} for the pressure dependence of the apparent propagation equilibrium constant ($K_{prop} = 1/[\text{myosin}_{critical}]$) is obtained from the plot that appears as an inset in Figure 2 according to

$$\Delta V = (RT\ \Delta \ln K_{prop})/\Delta P \qquad (1)$$

in which R = 8.2 cm^3 MPa mol^{-1} $°C^{-1}$, T is the absolute temperature, K_{prop} is the propagation equilibrium constant, and P is the pressure in megapascals (1 MPa = 10 atm).

Mean Filament Length and Structure at Atmospheric Pressure. A mean filament length of 0.65 μm (±0.07 μm), n = 124, was obtained by measuring cross-linked myosin filaments in the electron microscope. This measurement helps to characterize the experimental system and allows the relative length measurements obtained in the kinetic experiments to be related to an absolute value. An electron micrograph of a typical field of these characteristically bipolar filaments is shown in Figure 3.

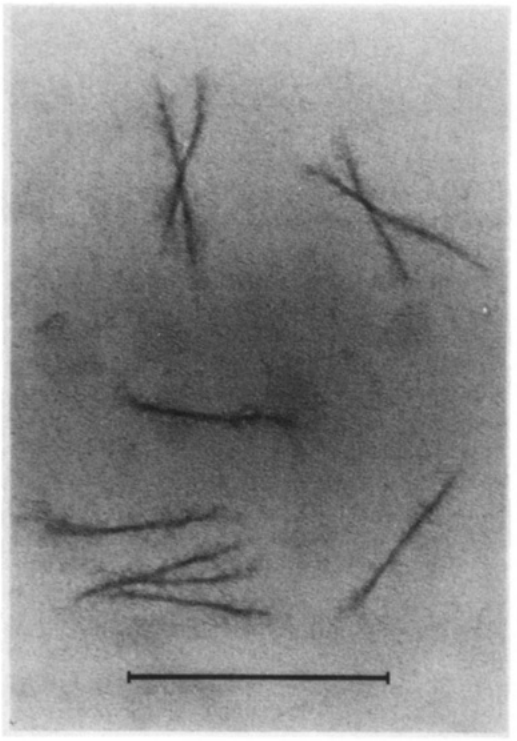

FIGURE 3: Electron micrograph of the bipolar filaments used in these experiments. The bar represents 1 μm.

Biphasic Kinetics and Their Analysis. The experimental requirements and rationale behind the analysis of the upward P-jump experiments on myosin filaments have been dealt with (Davis, 1981a,b). In what follows, a general mechanism (eq 2–5) is first presented for the sequential dissociation of a dimer from polymer and is then refined within the framework of the experimental constraints (eq 6–9) to provide four constants that fully described the two resolvable phases of the dissociation process.

$$F_n \xrightarrow{k_n} F_{n-1} + D$$

$$F_i \xrightarrow{k_i} F_{i-1} + D$$

$$F_2 \xrightarrow{k_2} 2D$$

$$d[F_{i-1}]dt = k_i[F_i] \quad (2)$$

Because of the bipolarity of myosin thick filaments

$$d[F_{i-1}]/dt = k_i[2F_i] \quad (3)$$

The experiments are carried out under pseudo-zero-order conditions with the filament concentration remaining constant for greater than 90% of the reaction. The observed pseudo-zero-order rate constant k'_i is defined

$$k'_i = k_i[2F_i] \quad (4)$$

The observed and actual dissociation rate constants k'_i or k_i have an exponential dependence on the number of dimer subunits present in the thick filament (Davis, 1981b); this is exemplified by the following relationship:

$$k_i = k_n e^{\alpha i} \quad (5)$$

α provides a measure of the cooperativity of the reaction were it monophasic in character.

At present, it is not possible to determine the number of dimer subunits present in a filament of a particular length, or for that matter to obtain the absolute concentration of the

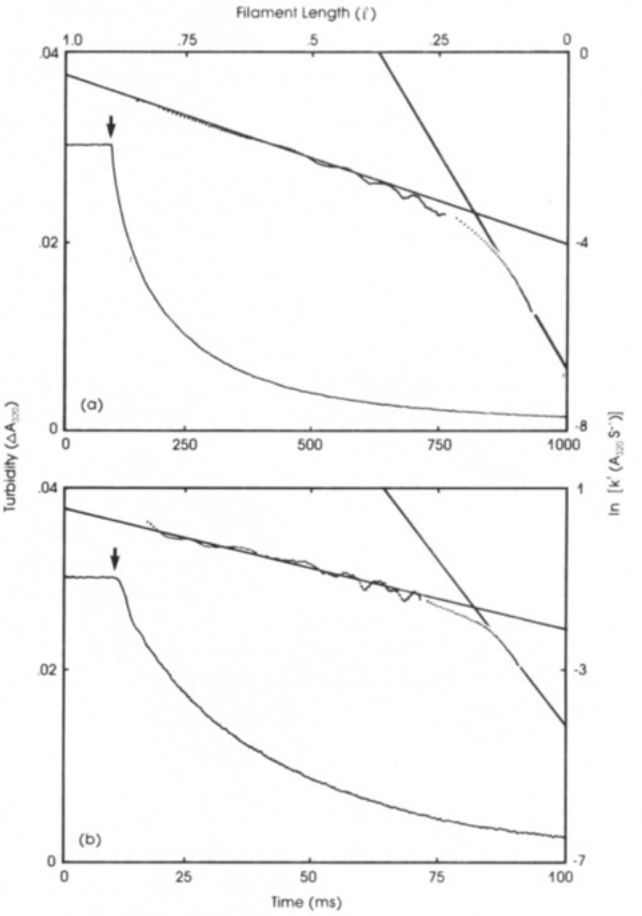

FIGURE 4: Complete dissociation of myosin filaments by a 3-ms stepwise increase in hydrostatic pressure. The myosin concentration used was 0.4 mg/mL. The amplitude of the pressure change at the point marked by the arrow was 17.5 MPa in (a) and 32.5 MPa in (b). The two linear phases of the secondary plot of the natural logarithm of the first derivative of the transient against length were used to obtain the kinetic constants.

filaments participating in the reaction. Other measures of these quantities had to be devised (Davis, 1981a,b). The mean length of a filament at time t during the dissociation reaction is operationally defined as $l = A_t/(A_0 - A_\infty)$. A problem arises, however, when the relationship of the subunits to each other changes over from the well-characterized parallel- to the less well-characterized antiparallel-packed mode of assembly. A consequence of this could well be a change in the specific turbidity for the incorporation of nonfilamentous myosin into the filament. This would introduce an error into the estimates of length. The only guideline here is that the small myosin minifilaments (containing ±18 myosin molecules) have an $A^{1\%}_{320}$ of 0.7 (albeit in a different solvent) (Reisler et al., 1980) compared to the $A^{1\%}_{320}$ of 1.50 for synthetic filaments.

The determination of the pseudo-zero-order rate constants by drawing tangents to the reaction profile to obtain the first derivative ($\Delta A_{320}/\Delta t$) at various filament lengths has been replaced by a computer-based method using a least-squares fit to a quadratic function (Savitzky & Golay, 1964). The filament length data are also smoothed. A 21-point fit to 900 data points was generally found suitable for analyzing the initial stages of a reaction while a 25-point fit to 90–180 selected points suited the latter part. The signal to noise ratio was improved by the computer averaging of nine similar transients in each case. Typical plots of these averaged data are shown in Figure 4.

Equation 5 is modified in the following way in order to accommodate the experimental constraints. The subscript l

defines the length of filament to which a particular rate constant pertains. The observed rate constants for the dissociation of the parallel-packed section of the thick filament are defined

$$k'_l = k'_1 e^{\alpha l} \quad (6)$$

The constant α gives a measure of the extent of cooperativity of the reaction and is routinely quoted in terms of a 10% change in length.

$$\alpha = (\ln k'_l - \ln k'_1)/[10(1 - l)] \quad (7)$$

The first 60% of the ln k'_1 against l plots shown in Figure 4 are linear and can be analyzed in the above manner. ln k'_1 is obtained by extrapolation back to the full length present at the start of the reaction.

The analysis of the second phase of the reaction (defined as the close to linear section between 85% and 92.5% dissociation of the ln k'_1 against l plots in Figure 4) in which antiparallel-packed myosin dissociates uses ln k'_0 (obtained by extrapolation to the limit of full dissociation) as the reference rate constant and β as a measure of cooperativity. The relationships are derived from eq 5 and are similar in form to eq 6 and 7 used in the analysis of the experiments on parallel-packed myosin.

$$k'_l = k'_0 e^{\beta l} \quad (8)$$

$$\beta = (\ln k'_0 - \ln k'_l)/10l \quad (9)$$

The mean dissociation rate constants, k'_1 and k'_0, have units of A_{320} per second. If need be, the units of k'_1 and α can be converted to absolute concentration values by using the specific turbidity for the incorporation of nonfilamentous myosin into the parallel-packed regions of the filament. This, as has been pointed out, cannot be done for k'_0 or β; it is, however, not a necessary condition for the conclusions that will be drawn from the concentration and pressure dependencies of k'_1, k'_0, α, and β in subsequent sections of the paper.

A measure of the relative extent of these two phases can be obtained by extrapolating the two log plots to a point of mutual intersection (see Figure 4) and noting the apparent filament length at which this occurs. The average value for this in all the experiments varies little and was $l = 0.20 \pm 0.02$ (SD), $n = 11$. This point of intersection, however, is only operationally defined and is dependent on the correctness of the relationship used to obtain the filament length and k'_0 from the turbidity data.

Validation of Pseudo-Zero-Order Conditions. It is essential to show that under the solvent conditions, the myosin concentrations, and the dissociation pressures used the pseudo-zero-order mechanism shown in eq 4 holds for the analysis of both phases. For these conditions to be met, k'_l must have a linear dependence on total myosin concentration ($k_l = k'_l/[2F_l]$) once it rises above the critical concentration (Josephs & Harrington, 1966). The plots of k'_1 and k'_0 against total myosin concentration in Figures 5 and 6, respectively, should therefore have the same form as the plot of turbidity against total myosin concentration (at atmospheric pressure) of Figure 2. The critical concentrations obtained from the intercepts with the concentration axes of Figures 2, 5, and 6 should as a consequence be similar; this is in fact so, with the values for the k'_1, k'_0, and A_{320} plots being 0.22, 0.21, and 0.20 mg/mL, respectively.

The cooperativity (α and β of eq 6 and 8) of the two phases of the reaction should be virtually concentration independent. This is because filament length (at atmospheric pressure)

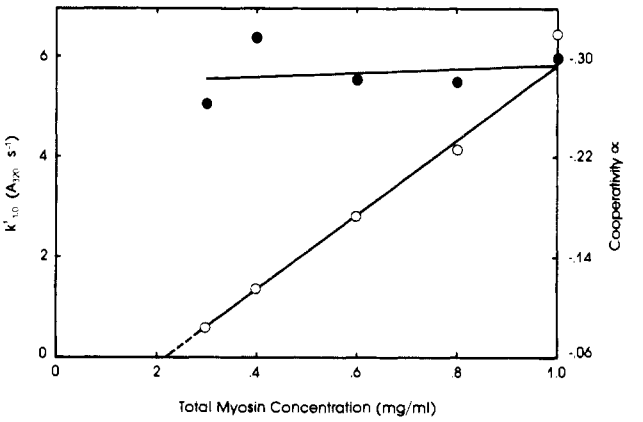

FIGURE 5: Effect of total myosin concentration on the rate of dissociation (○) of a full-length filament and the degree of cooperativity (●) of the parallel-packed segment of the thick filament. The pressure jump used was 27.5 MPa.

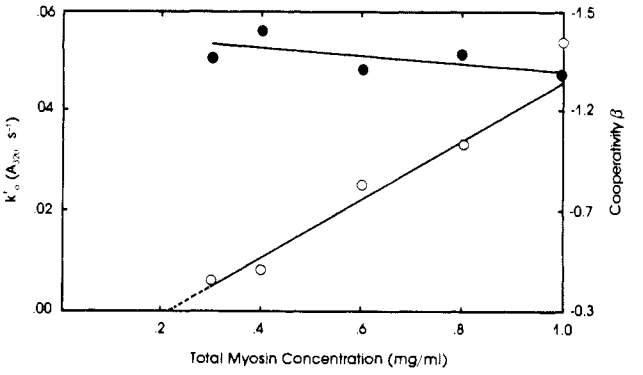

FIGURE 6: Effect of total myosin concentration on the apparent rate of dissociation at zero filament length (○) and the degree of cooperativity (●) of the antiparallel-packed region of the thick filament. The pressure jump used was 27.5 MPa.

depends on the concentration of nonfilamentous myosin, which as has been pointed out remains virtually constant above the critical concentration. A consequence of this is that thick filament size is buffered. The mechanisms and relationships underlying this are

$$M + M \underset{}{\overset{K_1}{\rightleftharpoons}} D + F_{i-1} \underset{k_{-i}}{\overset{k_2}{\rightleftharpoons}} F_i$$

$$k_{-i} = k_2 K_1 [M]^2 \quad (10)$$

An examination of Figures 5 and 6 shows both α and β to be, as far as can be judged, concentration independent.

Pressure Dependence of Dissociation Rate Constants. A useful indication of the extent of the charge–charge interactions that participate in the generation of the antiparallel- and parallel-packed zones of the thick filament (see Discussion) can be gained from the pressure dependence of the dissociation rate constants at different filament lengths. The extent of the cooperativity and rates of dissociation at atmospheric pressure can be calculated provided that the reaction mechanism remains unaltered by pressure. These rate data can be corrected to atmospheric pressure for direct correlation with the assembly kinetic data obtained at atmospheric pressure (Davis, 1981b). The pressure dependence of the rate of depolymerization of the parallel-packed myosin of the thick filament is shown in Figures 7 and 8. The dependence on pressure of the reaction is analyzed by means of a plot of ln k'_1 and α against P. Equation 11 is used where ΔV^* is the activation volume, R

$$\Delta V^* = -(RT\, \Delta \ln k)/\Delta P \quad (11)$$

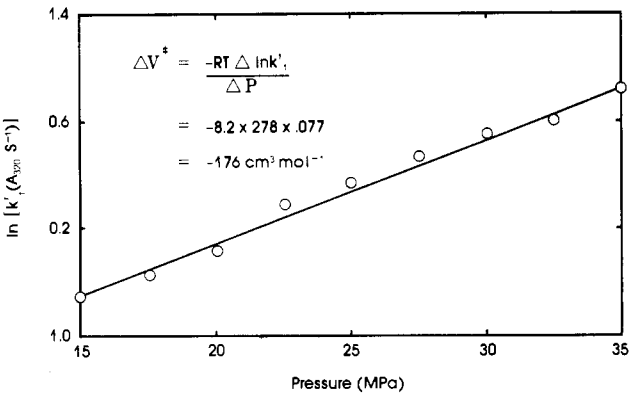

FIGURE 7: Effect of hydrostatic pressure on the natural logarithm of the observed dissociation rate constant for a full-length filament. The myosin concentration was 0.4 mg/mL.

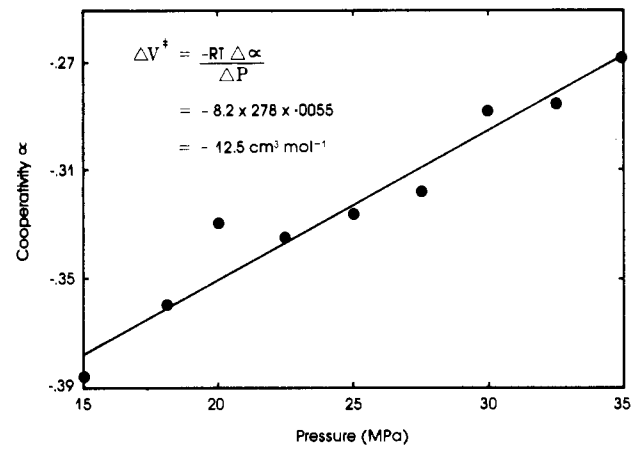

FIGURE 8: Effect of hydrostatic pressure on the cooperativity shown by parallel-packed myosin during the pressure-induced shortening of the thick filament. The myosin concentration was 0.4 mg/mL.

is 8.21 cm^3 MPa mol^{-1} $°C^{-1}$, T is the absolute temperature, k is the rate constant, and P is the pressure in megapascals. The pressure dependence of k'_1 gave a $\Delta V^{\ddagger}$ of -176 cm^3 mol^{-1} from an analysis of the data in Figure 7. The linearity of the plot points to the fact that the mechanism probably does not change with pressure. $\Delta V^{\ddagger}$ for the change in cooperativity with length can also be obtained thanks to the exponential dependence of k'_1 on length with the resultant linear dependence of $\Delta V^{\ddagger}$ on filament length. The data in Figure 8 gave a $\Delta V^{\ddagger}$ for α (the pressure sensitivity of the linkage between the individual dissociation rate constants) of -12.5 cm^3 mol^{-1}. The linearity of the plot once again underlines the stability of the sequential dissociation mechanism in general and to pressure to particular. $\Delta V^{\ddagger}$ therefore *decreases* with increasing length.

Data from the pressure dependence of k'_0 and β for the linear phase of the dissociation of the antiparallel-packed segment of the thick filament are analyzed in a similar manner to reactions involving parallel-packed myosin. The analysis of the linear plots in Figures 9 and 10 based on eq 11 gave a $\Delta V^{\ddagger}$ of -278 cm^3 mol^{-1} for k'_0 and a $\Delta V^{\ddagger}$ of 41 cm^3 mol^{-1} for β, once again indicating an apparently pressure-independent mechanism of reaction. $\Delta V^{\ddagger}$ *increases* with filament length, the antithesis of the situation with parallel-packed myosin discussed earlier.

$\Delta G°$ and Filament Length. The exponential increase in the dissociation rate constant with filament length for the two phases (assuming a length-independent association rate constant) implies that the Gibbs energy for the additon of dimer to the parallel-packed segment of the thick filament rises linearly as the filament grows. A model of this type has in

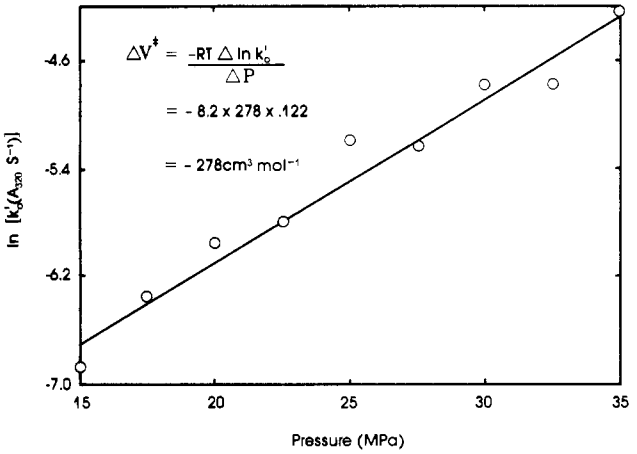

FIGURE 9: Effect of hydrostatic pressure on the natural logarithm of the observed dissociation rate constant for a zero-length filament. The myosin concentration was 0.4 mg/mL.

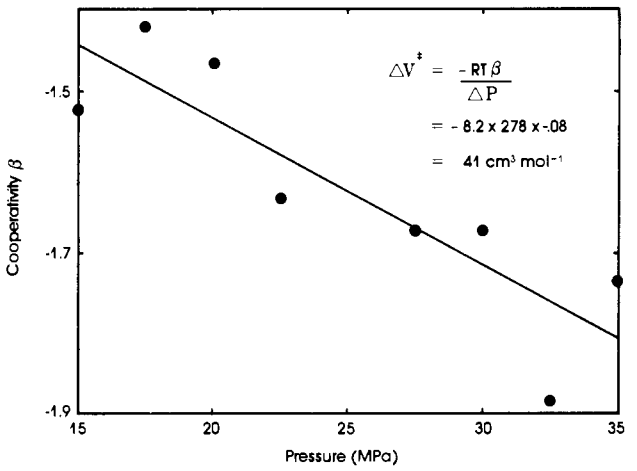

FIGURE 10: Effect of hydrostatic pressure on the cooperativity shown by a section of antiparallel-packed myosin during the pressure-induced shortening of the thick filament. The myosin concentration was 0.4 mg/mL.

fact been proposed as a basis for length regulation in polymers (Wagenknecht & Bloomfield, 1975). The $\Delta V^{\ddagger}$ for α, the cooperativity of the reaction, can be used to normalize the cooperativity data to atmospheric pressure by use of eq 11 [previous data were obtained at 15 MPa (Davis, 1981b)]. Since it has been shown that the reaction mechanism remains unaltered by changes in hydrostatic pressure, α has a normalized value of -0.459 for shortening filaments. The change in $\Delta G°$ for this process is obtained from the relationship:

$$\Delta G° = RT\alpha = -1.06\ \text{kJ mol}^{-1} \qquad (12)$$

It should be noted that the linearity of the relationship is not in question; the absolute measure of length may, however, be error prone.

The cooperativity data on the antiparallel-packed segment of the thick filament relate to an operationally but precisely defined section of this region. At this point, the assumption is made that the filament is assembled in a kinetically similar manner to the parallel-packed region, that is, from dimer at the maximum diffusion-limited rate (see Discussion). The cooperativity β has a value of -1.173 when normalized to atmospheric pressure using eq 11 and a $\Delta G°$ of -2.7 kJ mol^{-1} for a 10% decrease in filament length. If the specific turbidity of minifilaments is used as a measure of length (see the earlier discussion), the value for $\Delta G°$ would be roughly 20% lower.

No attempt has been made to calculate the overall con-

tribution to $\Delta G°$ of these two phases to the assembly of the thick filament due to the uncertainties over the extent of the individual reactions.

Discussion

It was mentioned in the introduction that electron microscope studies have revealed that the pH 8–8.5 filament class shares a number of structural features with the native filaments of vertebrate skeletal muscle; what now remains to be shown is that the molecular interactions between the individual subunits are similar under these two apparently different environmental conditions.

The first task here is to be clear as to what types of interaction predominate in the assembly of the thick filament. Fortunately, this is a relatively straightforward task as it has been realized for quite some time that charge–charge interactions undoubtedly play a central role in thick filament assembly. Evidence for this came originally from observations on the sensitivity of the myosin filament equilibrium to small changes in salt concentration and pH (Josephs & Harrington, 1968). Amino acid sequence data have since revealed that the rod section of the myosin molecule has a periodic distribution of charged amino acid residues along its length. Analysis of these data revealed that positive interactions between groupings of oppositely charged amino acid side chains on adjacent myosin molecules were favored at axial staggers of 14.3 and 42.9 nm, dimensions which correlate with the axial stagger of the subunits in the thick filament and of the myosin dimer, respectively (McLachlan & Karn, 1982, 1983). It is thus reasonable to suppose that if this information-rich pattern were altered, filament misassembly could result. It is clear that a change in pH or temperature would alter the charge pattern by affecting the cationic acid groups with pK values close to neutrality. In contrast, a change in salt concentration (apart from specific ion effects) would simply result in a generalized change in filament stability, leaving the charge pattern unaffected. It is thus important in the design of in vitro experiments to adjust the solvent pH to compensate for the effect of a change in temperature in order to maintain a physiological charge balance. The shift in the apparent pK for myosin from a body temperature (rabbit) of 39 °C and a pH of 7.2 to 5 °C (to prevent nonspecific aggregation) is 0.77 pH unit calculated from the apparent heat of ionization of 39.4 kJ mol^{-1} for myosin at pH 7.2 and 38 °C (Mihályi, 1950). A physiologically equivalent pH at 5 °C is accordingly 8 and not the decidely aphysiological pH of 7. In this context, it is intriguing to speculate that carnosine (β-alanyl-L-histidine), a major buffering component in frog muscle with a similar temperature dependence of its pK (Woledge, 1972) to the protein cationic acid groups (another important buffer component), could operate as a charge buffer for the protein components of muscle, and myosin in particular, as the temperature of the animals' environment changes.

ΔV^* values are generally considered to arise from changes in structure (e.g., bond breakage) and/or from changes in the extent of the solvation of the activated state vis-à-vis the reactants. When an ionic activated state is generated from neutral reactants, the volume decrease due to the electrostriction of solvent water about the charged groups is large and overshadows the generally small contribution from structural changes. The mechanistic interpretation of the ΔV^* values thus becomes relatively straightforward when charge generation plays a major role in a reaction. We can thus be reasonably confident that, in the case of myosin assembly, the degree of the pressure dependence of the dissociation rate constant will provide a direct measure of the extent of ionic interactions in the assembly of dimer into filament. The length dependence and the sign of $\Delta G°$ and ΔV^* can be used as an indication of the relative contribution of ionic as opposed to other types of noncovalent interactions in filament assembly. The contrasting results obtained from regions of parallel- as opposed to antiparallel-packed material can thus provide a valuable insight into the molecular interactions within the filament.

In the parallel-packed region, ΔV^* drops by 12.5 cm^3 mol^{-1} for each 10% change in length to reach a limiting and minimum value of −176 cm^3 mol^{-1} for the full-length filament. This means that ionic bonding between dimer and filament weakens progressively as the filaments grow. The change in the architecture of the dimer binding site at the tip of the growing filament thus reduces the availability of charge interaction in the assembly of dimer into filament. A mechanism for length regulation will therefore have to explain in physical–structural terms how this drop in charge–charge interaction comes about.

Antiparallel-packed myosin has its own characteristic properties. The interpretation of these data is somewhat complicated by not having precise kinetic data on the association reaction for antiparallel-packed myosin to show that the addition of dimer to filament is independent of polymer length. Pseudo-second-order kinetics do, however, appear to hold when the assembly reaction is initiated from filaments shortened by pressure to the extent that their lengths overlapped this zone (Davis, 1981b). This result indicates that dimer adds to the outer limits of the antiparallel-packed region at its diffusion-limited rate. There is also evidence to suggest that parallel dimer participates in the nucleation reaction. Support for this contention comes from experiments in which filamentogenesis was initiated de novo from salt-dissociated myosin. This reaction was analyzed as being pseudo first order with a second-order concentration dependence (Katsura & Noda, 1971, 1973). These workers interpreted their results as indicating that dimer participated in the propagation reaction. This is unlikely as a slow nucleation reaction followed by a significantly faster propagation reaction would exhibit a concentration dependence that relates to that of the reaction prior to the rate-limiting step, i.e., nucleation. The simplest kinetic model for interpretation of the results of Katsura and Noda would then be for a reaction in which a preequilibrium between myosin monomer and dimer was rapidly established followed by the dimer undergoing a rate-limiting first-order reaction in the nucleation step. It has been shown that rapidly formed parallel dimers are present in high concentrations under the conditions that promote filamentogenesis (Davis et al., 1982). It is thus very likely that parallel dimer is the species that participates in the first-order reaction. It therefore seems reasonable to conclude that, apart from the slow rate of reaction of parallel dimer in the unfavorable nucleation reaction, the remainder of the filament is generated by the assembly of parallel dimer at the diffusion-limited rate. It thus seems justifiable to interpret the kinetic and thermodynamic data in the same way as one did for parallel-packed myosin. The increase in $\Delta G°$ with length is somewhat greater than that for parallel-packed myosin ($\Delta G°$ = 2.7 kJ mol^{-1}) compared to 1.06 kJ mol^{-1} for a 10% change in the length for parallel-packed myosin. This enhanced stability is probably the direct result of the additional antiparallel interactions found in this region. Interestingly, the change in ΔV^* with length does not parallel the trend in the free energy of interaction in that its value rises by −41 cm^3 mol^{-1} from the limiting value of −278 cm^3 mol^{-1} for a zero-length filament. Ionic bonds thus become increasingly dominant as the filament grows and the interaction

with dimer progressively weakens; the contribution from other types of bonding therefore declines very sharply indeed. This points to the free-energy contribution from other types of noncovalent interactions being responsible for the enhanced stability of the region, particularly at short filament lengths.

The discovery of a progressive decrease in the $\Delta G°$ of interaction within a structure of comparable dimensions to that of the minifilament makes it unlikely that they function as a nucleus of the thick filament in the accepted sense of the word. As was pointed out, the reinterpretation of the experiments on de novo thick filament formation points to the nucleation reaction occurring between a pair of parallel dimers, an event which occurs very early in the assembly process. It remains to be discovered how this intermediate with its very high affinity for dimer is built.

It has recently been shown that different types of myosin molecules can be localized in different parts of the thick filament (Miller et al., 1983). This implies a selection mechanism of some sort. As we have seen, quite different bonding interactions occur in the parallel- and antiparallel-packed regions of the thick filament. A particular myosin variant might thus have a high affinity for assembly into the bare zone through a particular set of interactions and low affinity for assembly into the parallel-packed arms.

References

Cooper, J., & Trinick, J. (1984) *J. Mol. Biol. 177*, 137–152.
Davis, J. S. (1981a) *Biochem. J. 197*, 301–308.
Davis, J. S. (1981b) *Biochem. J. 197*, 309–314.
Davis, J. S. (1981c) *S. Afr. J. Sci. 77*, 499–500.
Davis, J. S. (1982) *J. Biochem. Biophys. Methods 6*, 61–69.
Davis, J. S. (1983) *Biophys. J. 41*, 299a.
Davis, J. S., & Gutfreund, H. (1976) *FEBS Lett. 72*, 199–207.
Davis, J. S., Buck, J., & Greene, E. P. (1982) *FEBS Lett. 140*, 293–297.
Josephs, R., & Harrington, W. F. (1966) *Biochemistry 5*, 3474–3487.
Josephs, R., & Harrington, W. F. (1968) *Biochemistry 7*, 2834–2847.
Katsura, I., & Noda, H. (1971) *J. Biochem. (Tokyo) 69*, 219–229.
Katsura, I., & Noda, H. (1973) *Adv. Biophys. 5*, 177–202.
Kellenberger, E. (1969) in *Symmetry and Function of Biological Systems at the Macromolecular Level* (Engstrom, A., & Strandberg, B., Eds.) pp 349–366, Wiley-Interscience, New York.
McLachlan, A. D., & Karn, J. (1982) *Nature (London) 299*, 226–231.
McLachlan, A. D., & Karn, J. (1983) *J. Mol. Biol. 164*, 605–626.
Mihyâlyi, E. (1950) *Enzymologia 14*, 224–236.
Miller, D. M., Ortry, I., Berliner, G. C., & Epstein, H. F. (1983) *Cell (Cambridge, Mass.) 34*, 447–490.
Reisler, E., Smith, C., & Seegan, G. (1980) *J. Mol. Biol. 143*, 129–145.
Savitzky, A., & Golay, M. J. E. (1964) *Anal. Chem. 36*, 1627–1639.
Starr, R., & Offer, G. (1971) *FEBS Lett. 15*, 40–44.
Wagenknecht, T., & Bloomfield, V. A. (1975) *Biopolymers 14*, 2297–2309.
Woledge, R. C. (1972) *Cold Spring Harbor Symp. Quant. Biol. 37*, 629–634.

Chromatin Structure of a 3-Methylcholanthrene-Induced Cytochrome P-450 Gene†

Leo Einck, John Fagan, and Michael Bustin*

Laboratory of Molecular Carcinogenesis, National Cancer Institute, National Institutes of Health, Bethesda, Maryland 20205

Received January 14, 1985

ABSTRACT: Plasmids carrying fragments of a cytochrome P-450 gene, inducible by 3-methylcholanthrene, were used to study the chromatin structure of this gene in the liver of normal and carcinogen-treated rats. Digestion with micrococcal nuclease revealed that the gene is not present in the typical 200 base pair nucleosomal structure. By use of indirect end-label hybridization, four DNase I hypersensitive sites were mapped in the 5′-terminal region of the gene. An S1 nuclease sensitive site is located close to a DNase I site. Gene induction by treatment with 3-methylcholanthrene does not result in detectable changes in the DNase I hypersensitive sites. Rat thymus chromatin does not contain DNase I hypersensitive sites in the P-450 gene, suggesting that in the liver the chromatin structure is altered so as to allow tissue-specific expression of the gene. This paper is the first study on the chromatin structure of a gene coding for a member of the cytochrome P-450 family of enzymes. The implications of our results to the understanding of gene regulation of the P-450 genes are discussed.

The cytochrome P-450 family of proteins is responsible for metabolizing a variety of xenobiotic and endogenous compounds including drugs, carcinogens, and toxins, (Conney, 1982). Some of the metabolites produced are potent mutagens and carcinogens which bind covalently to cellular macromolecules such as proteins, RNA, and DNA (Gelboin, 1980). Syntheses of the various members of the cytochrome P-450 enzyme system are highly inducible in a very selective manner, and the isoenzymes generated have distinct yet overlapping substrate specificities (Lu & West, 1980). Gene expression regulation, therefore, is central to the coordinate control of this family of genes.

Compared to total nuclear DNA, active or potentially active genes have an altered chromatin structure which can be examined with various nucleases [for a review of chromatin structure and nuclease sensitivity, see Igo-Kemenes et al. (1982) and Elgin (1981)]. Transcribable regions are preferentially digested with DNase I presumably because of an

† An abstract of this paper was presented at the Federation of American Societies for Experimental Biology Annual Meeting (Einck et al., 1985).

0006-2960/85/0424-5269$01.50/0